ARTICLES

Methyl Iodide Photodissociation at 193 nm: The I($^2P_{1/2}$) Quantum Yield

A. Gilchrist, G. Hancock, R. Peverall, G. Richmond, G. A. D. Ritchie,* and S. Taylor

Physical and Theoretical Chemistry Laboratory, Oxford University, South Parks Road, Oxford, OX1 3QZ, United Kingdom

Received: November 12, 2007; Revised Manuscript Received: March 3, 2008

Methyl iodide photolysis at 193 nm has been studied through probing the I($^2P_{1/2}$−$^2P_{3/2}$) transition in the atomic iodine photofragment using diode laser spectroscopy. The I($^2P_{1/2}$) quantum yield has been determined through two different diode laser techniques and then compared. Frequency-modulated diode laser based absorption spectroscopy was used to extract nascent Doppler lineshapes from which an I($^2P_{1/2}$) quantum yield of unity is inferred. However when diode laser gain/absorption measurements were made, an I($^2P_{1/2}$) quantum yield of 0.68 ± 0.04 was found. The reason for this discrepancy is shown to lie in the diode laser gain/absorption method. Molecular iodine is found to be formed during the experiment via atomic iodine recombination and then in turn dissociates to produce both I($^2P_{1/2}$) and I($^2P_{3/2}$), thus distorting the returned quantum yield. This conclusion is supported both by the reduction of the I($^2P_{1/2}$) quantum yield with number of photolysis laser shots when measured using this technique and by the presence of fluoresence which is shown to have excited-state lifetimes and quenching rates that are consistent with those previously measured for the D and D′ states of molecular iodine.

Introduction

The photolysis of alkyl iodides and their fluorinated counterparts provide benchmark systems upon which theory and experiments can be constructed.[1–7] There have been numerous studies concerned with exciting these species within the UV A band centered around 260 nm; these have included kinetic measurements, quantum yield determination of the electronically excited iodine atoms produced, through to full quantum state resolved studies extracting excited-state lifetimes and fragment angular distributions.[8–13] A wide and varied selection of techniques have been employed including laser-induced fluorescence (LIF),[14,15] resonant multiphoton ionization with time-of-flight detection (REMPI TOF),[16,17] velocity map ion imaging,[18] diode laser gain spectroscopy,[1,3] and photofragment translational spectroscopy.[19] Measurements within the second UV absorption band, known as the B band, involving excitation to higher-lying predissociative Rydberg states, are significantly less abundant, and work within this band has largely centered upon photolysis of methyl iodide and determining the excited-state lifetimes and their vibronic state dependence. The methyl photofragment has been the predominant focus of most of this work and has been probed though femtosecond photoionization spectroscopy[20,21] and REMPI-TOF.[22–25] and resonance Raman spectroscopy.[26,27] Emission studies[28] and some theoretical studies[29,30] have also been carried out on the photodissociation dynamics. Of particular relevance to this work is the discrepancy reported for the quantum yield for the production of I($^2P_{1/2}$) from the photolysis of methyl iodide at 193 nm. Hess et al.[23] directly probed the atomic iodine photofragment using diode laser gain vs absorption methods to determine the I($^2P_{1/2}$) (hereafter I*) quantum yield, which was found to be 0.70 ± 0.04. However, Van Veen et al.[31] and Continetti et al.[22] report unity quantum yields; though unlike Hess et al., in both these cases the values were inferred from TOF measurements that directly detected the CH_3 fragment. Van Veen et al. also determined the angular anisotropy, β, of the photofragments from the 193 nm photolysis of methyl iodide to be −0.72 ± 0.1. It is worth noting there have been no REMPI/TOF or ion imaging studies reporting directly probing the I($^2P_{3/2}$) (hereafter I) and I* photofragments that would provide a convenient and reliable alternative test of the I* quantum yield.

The B band of methyl iodide covers the wavelength region from 190 to 205 nm and is comprised of transitions resulting from the excitation of a nonbonding 5pπ electron situated purely on the I atom to a 6s molecular Rydberg orbital.[32] The remaining three 5pπ electrons exhibit strong spin−orbit coupling resulting in the ionic core comprising of $^2\Pi_{3/2}(^2E_{3/2})$ and $^2\Pi_{1/2}(^2E_{1/2})$ states when in C_{3v} symmetry. These states then couple with the Rydberg electron to give several bound states, two of which, Δ(E) and Π(E) arise from the $^2\Pi_{3/2}(^2E_{3/2})$ ionic core state, while states (Σ^+, Σ^-) (A_1, A_2) and Π(E) are due to the $^2\Pi_{1/2}(^2E_{1/2})$ ionic core state. The B band is comprised of excitation to the first two of these states, Δ(E) and Π(E), while the (Σ^+, Σ^-) (A_1, A_2) and Π(E) states collectively contribute to the C band. It has previously been seen that the perpendicular transitions to the Π(E) states dominate in both bands.[32] Curve crossing between these states and those of the A band result in predissociation, resulting in exit channels leading to $CH_3(^2A_2'')$ + I($^2P_{1/2}$) and $CH_3(^2A_2'')$ + I($^2P_{3/2}$) photofragments. At wavelengths between 140 and 170 nm C−H scission has previously been found to be the primary dissociation channel,[33] whereas literature on the VUV photodissociation at 121.6 nm reports two competing processes:[34,35] first a direct C−H scission and

* To whom correspondence should be addressed. E-mail: ritchie@physchem.ox.ac.uk. Phone: +44 1865 285723. Fax: +44 1865 275410.

10.1021/jp710799k CCC: $40.75
Published on Web 04/25/2008

second a two-step dissociation via either a stepwise dissociation of the internally excited methyl fragment or dissociation through a highly excited CH_3I intermediate. Continetti et al. found that this C−H scission channel contributed 3% of the total CH_3I dissociation at 193 nm.[22]

Previously we have studied the 266-nm photolysis of CF_3I and C_2F_5I using the time-resolved frequency modulated (FM) absorption technique, determining the nascent speed distribution and translational anisotropy parameter of the atomic iodine fragment.[1] In both these cases it is well established that the I* quantum yield is very close to unity, and as such the signals could be treated as pure gain. We now turn our attention to a system where there are conflicting reports of the quantum yield. A nonunity I* quantum yield would result in signals that are linear combinations of absorption and gain from the I and I* states. If this is the case the FM absorption technique employed, which is sensitive to the speed of both iodine fragments, can be used to resolve the contributions from I and I*. If there is no internal excitation of the methyl cofragment the ground-state iodine will be traveling at 800 ms^{-1} as compared to excited-state iodine at 700 ms^{-1}; as such the Doppler profile of the I will be 122 MHz wider than that of the I* Doppler profile. Furthermore the I and I* signals are absorption and gain in nature, respectively, and as such when coupled with differing widths, the high Doppler resolution afforded by the nascent FM technique enables resolution of the two speed components.

Experimental Section

The set up used for the transient studies with FM absorption spectroscopy is similar to that employed in our previous work.[1] The photofragments are generated from room-temperature flowing samples of methyl iodide (Aldrich, 99.5% purity) at pressures of ≈40 mTorr, using 193 nm radiation from an ArF Excimer laser (Lamda Physik COMPex 205) operating at 10 Hz, which is linearly polarized using a Rochon polarizer, with a pulse energy of 16 mJ prior to entering the reaction cell. The signal from a photodiode monitoring a partial reflection was used as a trigger for the data acquisition sequence.

The iodine photofragments were probed with hyperfine level, sub-Doppler resolution on the I*−I transition at 1315 nm using a distributed feedback (DFB) InGaAsP diode laser (Mitsubishi ML776H11F) with a bandwidth of ∼10 MHz. The near-IR radiation was focused through an electro-optic modulator (EOM) (Quantum Technology inc., 3500-P) to which a modulation frequency of 402 MHz was applied and then recollimated prior to passing through the reaction cell. Two Fabry−Perot etalons (Melles Griot 13SAE048) were used to control and monitor the spectral output of the probe laser. The laser was locked to a fixed etalon via a feedback circuit, with a second etalon operating in its scanning mode used to monitor the laser's spectral output.

Two reaction cells were used for this investigation, allowing use of the 3 experimental geometries illustrated in Figure 1. Geometries 1 and 2 utilize a simple glass photolysis cell, with a volume of 2×10^{-3} m^3, with the pump and probe beams arranged collinearly, while in geometry 3, the probe laser was multipassed across the pump beam path. The polarization of the probe beam was also rotated using a half-waveplate (B. Halle 700−2500 nm) giving full control over the angles θ and χ, as defined by Dixon.[36]

After exiting the reaction cell, the near-IR radiation was focused through an optical bandpass filter centered at 1315 nm (fwhm = 2 nm, Thorlabs) onto a fast InGaAs photodiode (1 GHz, New Focus). The detected signals were amplified (Minicircuits ZFL-500LN) and then demodulated with reference to the RF signal applied to the EOM in an RF demodulator circuit (Pulsar). The resulting In-phase (I) and Quadrature (Q) signals were filtered using two 39 MHz inline filters (Minicircuits SLBP-39) and recorded simultaneously using a Digital Storage Oscilliscope (DSO) (Tektronix TDS380).[37]

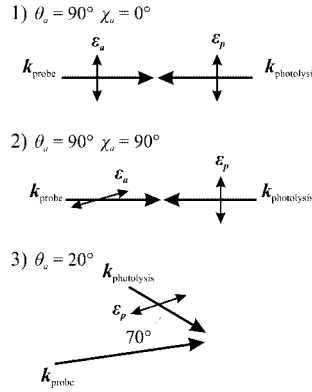

Figure 1. The three experimental geometries employed in the Doppler-resolved FM absorption experiments.

Results

Time-Resolved FM Doppler Absorption Measurements. To extract the nascent speed distribution, I* quantum yield, and the translational anisotropy parameter, the nascent pure FM absorption profile must be extracted. The method by which this is achieved is the same as that in our previous work.[1] First, a numerical integration over a series of time intervals with limits separated by 100 ns of the recorded I and Q signals was performed for a single diode laser frequency. The laser frequency detuning was calibrated from the monitor etalon signals where the separation of the sideband from the carrier frequency is equal to the modulation frequency. The frequency scale is then combined with the result from the integration to give I and Q signals at given times post photolysis. At later times (3.9−4 μs post photolysis) thermalization of the I and I* levels is sufficient to model the absorption profile with a Gaussian line shape. Through the Kramer−Kronig relations the associated dispersion line shape can therefore be determined, thus enabling the I and Q signals, which are linear combinations of absorption and dispersion related by the FM phase angle, θ, to be modeled. The late time I and Q signals can therefore be simultaneously fit in order to determine θ, in order to isolate the pure FM absorption signal. The nascent signals are then taken as those for 0 to 100 ns post photolysis.

The analysis of the Doppler-resolved transient lineshapes is based upon that of Hall and Wu.[39] By use of this description a linear combination of area normalized signals from the geometries shown in Figure 1 (denoted D_1, D_2 , and D_3, respectively) can be constructed to produce a Doppler profile that is solely dependent upon the speed distribution, $D_1 + D_2 + 1.21D_3$. The isotropic Doppler profile is a sum of two components, one resulting from I atom absorption and the other gain from I*. This isotropic profile is therefore described by the sum of two isotropic Doppler profiles of opposite sign

$$D_{iso} = wD_{I^*} - (1 - w)D_I \quad (1)$$

where w is the fraction of iodine atoms that are in the I* state. The I and I* Doppler profiles have different speed distributions, each of which is fitted to the following function[40]

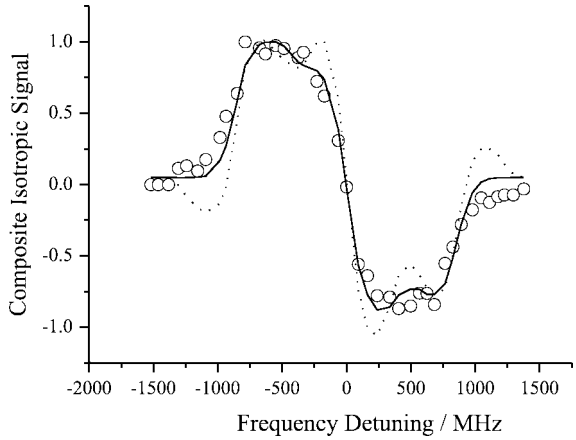

Figure 2. The composite isotropic Doppler profile for the nascent iodine photofragment (open circles). The fit from which the speed distribution is extracted is shown as a solid line; the fraction of I* is found to be 1.0 ± 0.15. The dotted line shows a simulation of the isotropic profile with a quantum yield for formation of I* of 0.70.

$$P(E_T) = E_{avail}[f_T^a(1-f_T)^b] \quad (2)$$

where f_T is the fraction of available energy in translation and a and b are dimensionless parameters that can be varied.

The isotropic composite profile and returned fit are shown in Figure 2 as open circles and a solid line, respectively, with a returned fraction of I* of 1.0 ± 0.15. The mean speed of the nascent I* fragment was found to be 650 ms^{-1}, corresponding to 91% of the available energy being partitioned into translation. The I* quantum yield previously determined via the gain vs absorption method of 0.70 ± 0.04[23] would suggest a component of the composite isotropic signal from I and the majority from I*. As discussed earlier, any component of the signal resulting from I would have a broader Doppler width due to the extra available kinetic energy; it would also be opposite in sign to that arising from I* as it is absorption in nature. Thus the I channel would be expected to manifest itself as "wings" on the isotropic Doppler profile. The dotted line in Figure 2 shows a simulated isotropic Doppler profile with an I* quantum yield of 0.70. While the wings are clearly visible on the simulation they are not evident in the experimental data. In principle, I fragments moving at a similar velocity to I* could be produced in conjunction with CH_3 with significant vibrational excitation. However, studies of the methyl fragment suggest that this is not the case.[21,22,31] Our data therefore suggests that the quantum yield of I* is essentially unity within the noise limits of our FM measurements, contrary to the conclusions from the gain vs absorption measurement.

The speed distribution returned from fitting the composite isotropic profile can then be used to find the translational anisotropy parameter, β, as detailed in previous work.[4] A value of −0.71 ± 0.09 was found, which is in excellent agreement with the value of −0.72 ± 0.1 found by Van Veen et al.[31] This value is consistent with the excitation at 193 nm proceeding via a perpendicular transition as assigned by Mulliken and Teller,[32] where the deviation from the limiting value of −1 can be attributed to parent rotation post excitation but prior to dissociation. This effect can be quantified using eq 3 derived by Busch and Wilson, based upon the rotation of the parent molecule during dissociation of an excited bound state[41]

$$\beta = 2\{[P_2(\alpha) + \psi^2 - 3\psi \sin\alpha \cos\alpha]/(1+4\psi^2)\}P_2(\beta_0) \quad (3)$$

Here ψ is the angle of rotation of the molecule during the lifetime of the bound excited state, α the angle of rotation of the molecule during the lifetime of the dissociative state, and β_0 the limiting value of the translational anisotropy of the dissociation. The lifetime of the initially excited Π(E) bound state is 0.15 ps,[31] while the rotational period of methyl iodide is 3.3 ps,[31] giving ψ to be 0.29 rad. The lifetime of the (E,1) dissociative state to which the Π(E) state is coupled is 0.07 ps,[42] and therefore assuming the same rotational lifetime, α is 0.13 rad. Thus the result of this calculation yields a value of β = −0.76, in close agreement with the measured value.

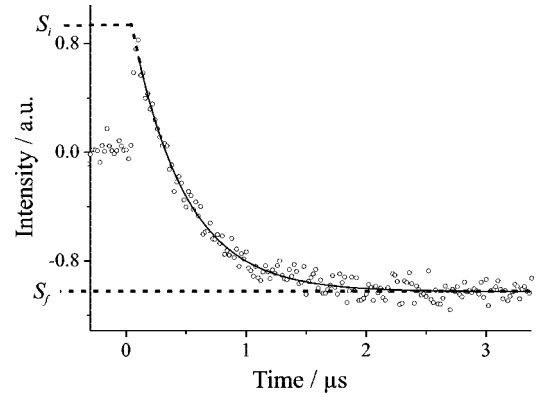

Figure 3. A typical diode laser gain vs absorption signal taken with a static gas mixture of 2 Torr CH_3I, 1.7 Torr O_2, and 43 Torr Ar. The initial and maximum gain signal is denoted S_i, and the final signal, at which point all I* initially produced has been quenched to I, is labelled S_f. The data returns an I* quantum yield of 0.68 ± 0.04.

Overall the results returned from the transient FM absorption data strongly suggest the I* quantum yield is 1.0 in agreement with Van Veen et al.[31] but in disagreement with Hess et al.[23]

Discussion

Discrepancies in the Quantum Yield. To confirm the near unity quantum yield returned from the transient FM absorption results further experiments to determine the I* quantum yield were carried out. Diode laser gain vs absorption measurements on the iodine photofragment were made in a similar manner to those previously carried out by Hess et al.[23]

The experimental setup used for these diode laser gain vs absorption measurements employs geometry 1, as shown in Figure 1. After the reaction cell, the unmodulated 1315 nm diode laser radiation is focused onto a fast photodiode (Thorlabs DET210). The probe laser is tuned to the center of the I*(F = 4) – I(F = 3) transition and then stepped off and on the transition 10 times, averaging the signal for 10 photolysis shots in each case. The off-resonance signals are taken as the background and are subtracted from the on-resonance traces. In this case a static gas sample consisting of 2 Torr of CH_3I, 1.7 Torr of O_2, and 40 Torr of Ar is used. Molecular oxygen is an efficient electronic quencher of I* due to a near resonant electronic transfer between the spin−orbit states of iodine and the $O_2(^3\Sigma_g^-)$and $O_2(^1\Delta_g)$ states, while Ar is used to ensure that both I and I* are translationally thermalizd so that the I and I* absorption and gain profiles have the same line shape.

A typical gain vs absorption signal, representative of those taken in the course of these experiments is shown in Figure 3. The initial and net gain signal, denoted S_i, is proportional to the population difference of the I and I* atoms initially produced. Over time the gain component decreases as the I* is electronically quenched to I, and thus the absorption signal increases with time. S_f is the value of the signal at long times (t > 30 μs); the signal at this point is purely absorption and as such is

proportional to the total number of I and I* atoms initially produced in the dissociation. The I* quantum yield is simply given by[38]

$$\Phi = \frac{1}{3}\left[\frac{S_i}{S_f} + 1\right] \quad (4)$$

The extracted values of S_i and S_f give a quantum yield of 0.68 ± 0.04 after 10 photolysis shots, which is in agreement with the value of 0.70 ± 0.04 found by Hess et al. using the same laser gain vs absorption method outlined above, with a similar number of averages.[23] Our experiments were carried out with a static sample at a total pressure of ~45 Torr. There were two noteworthy observations made in the course of carrying out this experiment. First a blue-green fluorescence was observed in the cell; second the quantum yield was found to vary with the number of shots over which the signal was averaged.

The disagreement in the I* quantum yield found not only in the literature but also within the experiments presented here must be a manifestation of an experimental effect within one of the two setups employed. It is proposed that a competing process is occurring in the reaction cell during the gain vs absorption measurements, which we recall were carried out under static conditions, and it is this process that is responsible for the conflicting results. We have previously noted that during the diode laser gain vs absorption measurements a blue-green fluorescence was observed in the cell; we now consider the origin of this fluorescence.

A reasonable hypothesis is that molecular iodine is formed via iodine atom recombination, which then in turn absorbs 193 nm radiation, redissociating to give both I and I*. Iodine atom recombination proceeds efficiently in the static gas mixture with the argon acting as a third body thus producing significant amounts of molecular iodine.[43,45] Molecular iodine has a large absorption cross section, ~1.7×10^{-17} cm^2, in the region of 180−200 nm,[46] which results, for 193 nm radiation, in excitation to the $v = 149$ vibrational level of the D($^1\Sigma_u^+$) state. This state can then undergo fluorescence at 193 nm, vibrational relaxation followed by fluorescence at 325 nm, or collisional relaxation to the D′($^3\Pi_{2g}$) state, as illustrated in Figure 4.[47,48] The D′ state can likewise undergo quenching processes and emit fluorescence between 340 and 510 nm. The discrepancy in the quantum yield findings may then be explained if the laser gain vs absorption method not only measures the I* quantum yield from the CH_3I dissociation but also that from molecular iodine dissociation. In this case the I* quantum yield would be expected to change with successive laser shot number as the concentration of molecular iodine increases during an experiment; conversely if the atomic iodine is produced solely from methyl iodide, the quantum yield should remain constant. The first of these cases fits with our previous observation that the quantum yield varied with number of photolysis shots over which the signal was recorded.

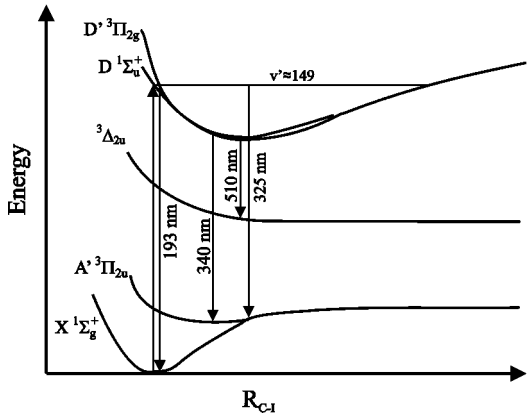

Figure 4. A schematic representation of the molecular iodine states involved following excitation at 193 nm.[50]

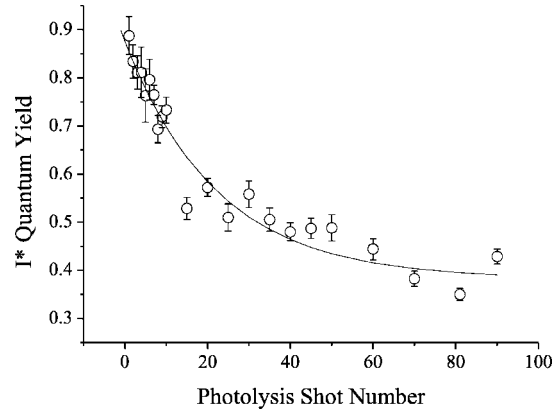

Figure 5. The variation of the quantum yield determined via the diode laser gain vs absorption method with the number of photolysis (193 nm) laser shots on a static gas sample. Note that the solid line is a guide to illustrate the decreasing trend.

The laser gain vs absorption measurements were therefore repeated, recording the signal after each successive dissociation laser pulse. These signals were fitted and the quantum yield extracted. As shown in Figure 5, the quantum yield decays with shot number and can be attributed to the increasing molecular iodine concentration in the static sample over the course of the experiments, which dissociates to give both I and I* thus changing the quantum yield. We note that the quantum yield on the first photolysis shot in Figure 5 is not unity; this is the case as, for the static conditions employed, there is always some residual molecular iodine stuck to the wall of the reaction cell which contributes to the signal even on the first photolysis shot.

To further confirm the presence of molecular iodine the fluorescence signals were investigated. The time-resolved emission was measured directly using a photodiode (Thorlabs DET210) for static samples comprising of 200 mTorr of methyl iodide and either oxygen or argon at pressures between 0 and 100 Torr. The fluorescence signals were modeled using the literature values for the radiative lifetimes of the D and D′ states, 15.5 ns[48] and 9.5 ns,[49] respectively, and the collisional relaxation rate coefficients,[50] convolved with the temporal pulse shape of our 193 nm laser. Figure 6 shows an example of the comparison between a simulated signal and that recorded in the experiments. There can be seen to be good agreement, consistent with I_2 being present in the gas mixture. The time-resolved fluorescence signals are dominated by the 25 ns photolysis pulse due to the short radiative lifetimes of the D and D′ states, with the rate of decay of the fluorescence relatively insensitive to the Ar or O_2 pressure and their respective quenching rate constants.

The fluorescence intensity was found to decrease with increasing O_2 pressure but increase with Ar pressure. Oxygen efficiently collisionally quenches the D state to the D′ state, and likewise the D′ state to nonradiative states.[50] Thus as the pressure of molecular oxygen increases, the rate at which population is removed to nonradiative states increases, and in turn a decrease in the fluorescence intensity is seen. Argon, however, efficiently quenches the D state to the D′ state but unlike O_2 is a significantly less efficient quencher of the D′ state.[50] Thus the relatively high rate of transfer into, coupled

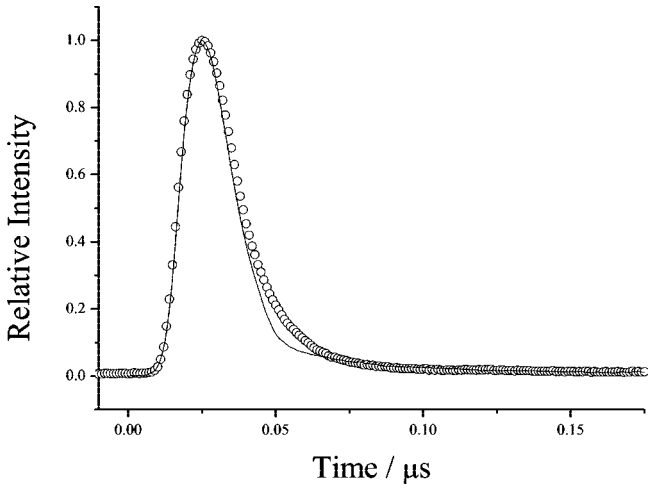

Figure 6. The measured and simulated fluorescence signals with a static gas sample of 0.2 Torr CH_3I and 101.2 Torr Argon.

with the extremely low level of quenching out of, the D′ state results in increasing I_2 fluorescence with increasing Ar pressure as population is pooled in the fluorescent D′ state. A further effect is the catalysis of iodine atom recombination to form molecular iodine by both oxygen and argon which acts to increase the rate of I_2 production as a function of pressure for both species leading to increased fluorescence intensity.[43,44,51]

Argon itself does not absorb at 193 nm; however, the Schumann−Runge bands of $O_2(B^3\Sigma_g^- - X^3\Sigma_g^-)$ encompass this wavelength region. If fluorescent transitions originating from these bands dominated, the signal intensity would be expected to increase with pressure of O_2, the opposite trend to that observed. No fluorescence is observed in the absence of CH_3I, and we can therefore discount any contribution to the fluorescence from the molecular oxygen present. It is also worth noting, despite the excess of O_2 present, effects resulting from its absorption of 193 nm radiation will be reduced due to its relatively small absorption cross section of 2×10^{-21} cm^2 [52] as compared to that of 1.7×10^{-17} cm^2 [46] for I_2.

Previous quantum yield measurements made using the laser gain vs absorption method on alkyl iodides have been made in the A band region.[7] The returned I* quantum yield values for various compounds in this photolysis band between 240 and 320 nm are in good agreement with those found via other techniques including those on the alkyl cofragment.[5,6] Such consistency between different techniques may be explained by the lower I_2 absorption cross section, 8.14×10^{-19} cm^2 molecule^{-1} [53] at 266 nm, compared to 1.7×10^{-17} cm^2 molecule^{-1} [46] at 193 nm. In contrast, the alkyl iodide absorption cross sections are of the same order in both the A and B photolysis bands, 9.2×10^{-19} cm^2 molecule^{-1} and 1.2×10^{-18} cm^2 molecule^{-1}, respectively,[54] and thus the photolysis of molecular iodine at these longer wavelengths is insignificant compared to the alkyl iodide photolysis in the first UV photolysis band.

Conclusion

The quantum yield for the formation of I* from the 193 nm photolysis of methyl iodide has been investigated using two techniques, with each method returning a different value. While the value of 0.68 ± 0.04 returned using the laser gain vs absorption method is in close agreement with a previous study by Hess et al.,[23] we believe that the true I* quantum yield is essentially unity, as found using the Doppler-resolved FM absorption method and in previous studies probing the methyl fragment directly.[22,23] The I* quantum yield has been shown to decay with laser shot number when measured using the diode laser gain vs absorption method, providing evidence for an accumulation of another species formed during the course of the experiments. Fluorescence was observed under the conditions of the laser gain vs absorption experiments though not in the Doppler-resolved FM measurements. Investigation of the fluorescence signals provides evidence for the presence of molecular iodine. It can therefore be concluded that the diode laser gain vs absorption technique on the I photofragment is compromised by the production of molecular iodine, which subsequently dissociates providing a secondary route for the production of both I and I*.

The significantly lower pressures of a flowing gas sample used in the nascent FM experiments result in a very slow iodine atom recombination rate, allowing little time for any molecular iodine produced to accumulate in the cell. The nascent FM profiles can therefore be confidently taken to represent only the iodine photofragment from methyl iodide photolysis. The near unity I* quantum yield extracted by this method is in agreement with that found by previous studies carried out on the methyl fragment, which would be unaffected by the production of any molecular iodine. We can therefore confidently extract the translational anisotropy parameter, β, of I* atoms from the photolysis of methyl iodide at 193 nm using the Doppler-resolved FM absorption technique; β was found to be -0.71 ± 0.09, and its deviation from its limiting value of -1 can be quantitatively explained by rotation of the parent molecule post excitation but prior to dissociation.

Acknowledgment. This work was supported by the EPSRC (Portfolio partnership scheme LASER) and by the Leverhulme Trust (GR). G.A.D.R. is grateful to the Royal Society for a University Research Fellowship, and S.T. is grateful to DIAC for the award of a studentship.

References and Notes

(1) Hancock, G.; Hutchinson, A.; Peverall, R.; Richmond, G.; Ritchie, G. A. D.; Taylor, S. *Phys. Chem. Chem. Phys.* **2007**, *9*, 2234–2239.
(2) Ogorzalek, R.; Hall, G. E.; Haerri, H,-P.; Houston, P. L. *J. Phys. Chem.* **1988**, *92*, 5–8.
(3) Knee, L.; Khundkar, L. R.; Zewail, A. H. *J. Chem. Phys.* **1985**, *83*, 1996–1998.
(4) Cline, J. I.; Taatjes, C. A.; Leone, S. R. *J. Chem. Phys.* **1990**, *93*, 6543–6553.
(5) Donohue, T.; Wiesenfeld, J. R. *J. Chem. Phys.* **1975**, *63*, 3130–3135.
(6) Baklanov, A. V.; Aldener, M.; Lindgren, B.; Sassenberg, U. *Chem. Phys. Lett.* **2000**, *325*, 399–404.
(7) Hess, W. P.; Kohler, S. J.; Haugen, H. K.; Leone, S. R. *J. Chem. Phys.* **1986**, *84*, 2143–2149.
(8) Guo, H. *Chem. Phys. Lett.* **1991**, *187*, 360–366.
(9) Guo, H.; Schatz, G. C. *J. Chem. Phys.* **1990**, *93*, 393–402.
(10) Gedanken, A.; Rowe, M. D. *Chem. Phys. Lett.* **1975**, *34*, 39–43.
(11) Shapiro, M.; Bersohn, R. *J. Chem. Phys.* **1980**, *73*, 3810–3817.
(12) Baughcum, S. L.; Leone, S. R. *J. Chem. Phys.* **1980**, *72*, 6531–6545.
(13) Eppink, A.T.J.B.; Parker, D. H. *J. Chem. Phys.* **1999**, *110*, 832–844.
(14) Kavita, K.; Das, P. K. *J. Chem. Phys.* **2002**, *117*, 2038–2044.
(15) Gerck, E. *J. Chem. Phys.* **1983**, *79*, 311–315.
(16) Kang, W. K.; Jung, K. W.; Kim, D-C.; Jung, K-H. *J. Chem. Phys.* **1996**, *104*, 5815–5820.
(17) Person, M. D.; Kash, P. W.; Butler, L. J. *J. Chem. Phys.* **1991**, *94*, 2557–2563.
(18) Aguirre, F.; Pratt, S. T. *J. Chem. Phys.* **2003**, *118*, 1175–1183.
(19) Felder, P. *Chem. Phys.* **1991**, *155*, 435–445.
(20) Baronavski, A. P.; Owrutsky, J. C. *J. Chem. Phys.* **1998**, *108*, 3445–3452.
(21) Janssen, M. H. M.; Dantus, M.; Guo, H.; Zewail, A. H. *Chem. Phys. Lett.* **1993**, *214*, 281–289.

(22) Continetti, R. E.; Balko, B. A.; Lee, Y. T. *J. Chem. Phys.* **1988**, *89*, 3383–3384.
(23) Hess, W. P.; Naaman, R.; Leone, S. R. *J. Phys. Chem.* **1987**, *91*, 6085–6087.
(24) Dobber, M. R.; Buma, W. J.; de Lange, C. A. *J. Chem. Phys.* **1993**, *99*, 836–853.
(25) Syage, J. A. *Chem. Phys. Lett.* **1993**, *212*, 124–128.
(26) Wang, P. G.; Zhang, Y. P.; Ziegler, L. D. *J. Chem. Phys.* **1990**, *92*, 2806–2817.
(27) Ziegler, L. D.; Chung, Y. C.; Wang, P. G.; Zhang, Y. P. *J. Phys. Chem.* **1990**, *94*, 3394–3403.
(28) Lao, K.; Person, M. D.; Chou, T.; Butler, L. J. *J. Chem. Phys.* **1988**, *89*, 3463–3469.
(29) Donaldson, D. J.; Child, M. S.; Vaida, V. *J. Chem. Phys.* **1988**, *88*, 7410–7417.
(30) Guo, H. *Chem. Phys. Lett.* **1992**, *193*, 527–531.
(31) Van Veen, G. N. A.; Baller, T.; De Vries, A. E. *Chem. Phys.* **1985**, *97*, 179–186.
(32) Mulliken, R. S.; Teller, E. *Phys. Rev.* **1942**, *61*, 283–296.
(33) Levy, M. R.; Simons, J. P. *J. Chem. Soc., Faraday Trans. 2* **1975**, *71*, 561–570.
(34) Amaral, G.; Xu, K.; Zhang, J. *J. Phys. Chem. A* **2001**, *105*, 1115–1120.
(35) Tonokura, K.; Mo, Y.; Matsumi, Y.; Kawasaki, M. *J. Phys. Chem.* **1992**, *96*, 6688–6693.
(36) Dixon, R. N. *J. Chem. Phys.* **1986**, *85*, 1866–1879.
(37) Costen, M. L.; North, S. W.; Hall, G. E. *J. Chem. Phys.* **1999**, *111*, 6735–6749.
(38) Haugen, H. K.; Weitz, E.; Leone, S. R. *J. Chem. Phys.* **1985**, *83*, 3402–3412.
(39) Hall, G. E.; Wu, M. *J. Phys. Chem.* **1993**, *97*, 10911–10919.
(40) North, S. W.; Marr, A. J.; Furlan, A.; Hall, G. E. *J. Phys. Chem. A* **1997**, *101*, 9224–9232.
(41) Busch, G. E.; Wilson, K. R. *J. Chem. Phys.* **1972**, *56*, 3638–3654.
(42) Dzvonik, M.; Yang, S.; Bersohn, R. *J. Chem. Phys.* **1974**, *61*, 4408–4421.
(43) Blake, J. A.; Burns, G. *J. Chem. Phys.* **1971**, *54*, 1480–1486.
(44) Beck, W. H.; Mackie, J. C. *Chem. Phys. Lett.* **1976**, *44*, 444–448.
(45) Bunker, D. L.; Davidson, N. *J. Am. Chem. Soc.* **1958**, *80*, 5085–5090.
(46) Myer, J. A.; Samson, J. A. R. *J. Chem. Phys.* **1970**, *52*, 716–718.
(47) Hemmati, H.; Collins, G. J. *Chem. Phys. Lett.,* **1979**, *67*, 5–8.
(48) Callear, A. B.; Erman, P.; Kurepa, J. *Chem. Phys. Lett.* **1976**, *44*, 599–601.
(49) Jewsbury, P. J.; Lawley, K. P.; Ridley, T.; Al-Adel, F. F.; Langridge-Smith, P. R. R.; Donovan, R. J. *Chem. Phys.* **1991**, *151*, 103–109.
(50) Exton, R. J.; Balla, R. J. *J. Quant. Spec. Rad. Transfer* **2004**, *86*, 267–283.
(51) Boriev, I. A.; Gordon, E. B. *Chem. Phys. Reports* **1998**, *17*, 1257–1265.
(52) Yoshino, K.; Freeman, D. E.; Esmond, J. R.; Parkinson, W. H. *Planet Space Sci.* **1983**, *31*, 339–353.
(53) Saiz-Lopez, A.; Saunders, R. W.; Joseph, D. M.; Ashworth, S. H.; Plane, J. M. C. *Atmos. Chem. Phys.* **2004**, *4*, 1443–1450.
(54) Fahr, A.; Nayak, A. K.; Kurylo, M. J. *Chem. Phys.* **1995**, *197*, 195–203.

JP710799K